

Discriminating soil crust type, development stage and degree of disturbance in semiarid environments from their spectral characteristics

S. CHAMIZO^a, A. STEVENS^b, Y. CANTÓN^c, I. MIRALLES^a, F. DOMINGO^a & B. VAN WESEMAEL^b

^aDepartamento de Desertificación y Geo-Ecología, Estación Experimental de Zonas Áridas, CSIC, 04120 Almería, Spain, ^bGeorges Lemaître Centre for Earth and Climate Research, Earth and Life Institute, Université Catholique de Louvain, 1348 Louvain-La-Neuve, Belgium, and ^cDepartamento de Edafología y Química Agrícola, Universidad de Almería, 04120 Almería, Spain

Summary

Biological soil crusts (BSCs) are increasingly recognized as common features in arid and semiarid ecosystems and play an important role in the hydrological and ecological functioning of these ecosystems. However, BSCs are very vulnerable to, in particular, human disturbance. This results in a complex spatial pattern of BSCs in various stages of development. Such patterns, to a large extent, determine runoff and erosion processes in arid and semiarid ecosystems. In recent years, visible and near infrared (Vis-NIR) diffuse reflectance spectroscopy has been used for large-scale mapping of the distribution of BSCs. Our goals were (i) to demonstrate the efficiency of Vis-NIR spectroscopy in discriminating vegetation, physical soil crusts, various developmental stages of BSCs, and various types of disturbance on BSCs and (ii) to develop a classification system for these types of ground cover based on Vis-NIR spectroscopy. Spectral measurements were taken of vegetation, physical crusts and various types of BSCs prior to, and following, trampling or removal with a scraper in two semiarid areas in SE Spain. The main spectral differences were: (i) absorption by water at about 1450 nm, more intense in the spectra of vegetation than in those of physical crusts or BSCs, (ii) absorption features at about 500 and 680 nm for the BSCs, which were absent or very weak for physical crusts, (iii) a shallower slope between about 750 and 980 nm for physical crusts and early-successional BSCs than for later-successional BSCs and (iv) a steeper slope between about 680 and 750 nm for the most developed BSCs. A partial least squares regression-linear discriminant analysis of the spectral data resulted in a reliable classification (Kappa coefficients over 0.90) of the various types of ground cover and types of BSC disturbance. The distinctive spectral features of vegetation, physical crusts and the various developmental stages of BSCs were used to develop a classification system. This will be a promising tool for mapping BSCs with hyperspectral remote sensing.

Introduction

Abiotic or physical soil crusts are compacted surface layers ranging from several millimetres to several centimetres in thickness and frequently found in arid and semiarid regions. Under adequate conditions of climate and soil stability, bare soils and physical crusts are colonized by microorganisms, gradually forming biological soil crusts (BSCs), which are an association of soil particles with cyanobacteria, algae, microfungi, lichens and bryophytes. Within the succession of BSCs in arid and semi-arid regions, cyanobacteria are the first colonizers. Polysaccharides exuded by cyanobacteria bind soil particles together (Verrecchia *et al.*, 1995),

stabilizing the soil surface and permitting later colonization by lichens and mosses (Belnap, 2006).

Biological soil crusts are widespread in arid and semiarid ecosystems and play an important role in the hydrological and ecological functioning of these ecosystems. They alter many soil surface characteristics affecting surface runoff and, thereby, the distribution and colonization of vascular plants (Belnap, 2006). They also increase soil stability and reduce wind and water erosion by protecting the soil against raindrop impact and the erosive force of wind (Maestre *et al.*, 2011). However, some studies indicate that BSCs lead to increased runoff (Zhan & Miller, 1996). The effect of this additional runoff on erosion should be evaluated on larger spatial scales to assess the combined impact of these effects and the potential for water harvesting from crusted areas

Correspondence: S. Chamizo. E-mail: schamizo@eeza.csic.es

Received 3 August 2010; revised version accepted 22 September 2011

to nourish adjacent vegetated areas (Cantón *et al.*, 2011). A tool able to estimate the spatial distribution of BSCs at hillslope and catchment scale would be required for establishing such effects. Furthermore, BSCs have been demonstrated to be very vulnerable to disturbances such as tracked-vehicle traffic, grazing and trampling by livestock, especially in soils with limited aggregate stability. The loss or disturbance of BSCs is one of the factors leading to accelerated soil erosion and other forms of land degradation (Belnap, 1995). The protection offered by BSCs prevents soil and nutrient loss, which can rapidly be exacerbated following disturbance to a crust. Therefore, it is important to identify the distribution of BSCs and monitor their spatial and temporal changes (Chen *et al.*, 2005).

In recent years, proximal and remote sensors measuring the visible and near infrared (Vis-NIR; 350–2500 nm) reflectance of soils have been exploited for detecting, mapping and monitoring BSCs. Some attempts at mapping crusts from field and remote sensing data have been made, to include soil crusting as an input parameter in runoff and erosion models. However, these have been mainly restricted to physical crusts (Cerdan *et al.*, 2001; King *et al.*, 2005). As input parameters in runoff and erosion models, biological crust-covered surfaces have so far only been mapped from morphological descriptions in the field for small areas (Cantón *et al.*, 2002). The potential of spectroscopy for mapping soil crusts has been reported in a few publications. Ben-Dor *et al.* (2004) showed that physical crusts can be spectrally modelled. The spectral characteristics of BSCs have been analysed by several authors (Karnieli *et al.*, 1999; Chen *et al.*, 2005; Weber *et al.*, 2008) and several indices, such as simple combinations of spectral bands, have been tested for mapping BSCs from hyperspectral images. Karnieli (1997) developed an index to separate cyanobacteria-dominated BSCs from bare sand. Chen *et al.* (2005) developed an index to differentiate lichen-dominated BSCs from bare soil and plants. Weber *et al.* (2008) developed an index to distinguish BSCs (mainly dominated by cyanobacteria) from surfaces devoid of BSCs. However, a universal method to distinguish between BSCs and other types of cover has not yet been developed (Karnieli *et al.*, 2003), nor has an index applicable to different ecosystems been proposed. Moreover, a methodology to distinguish different types of BSCs, ranging from early-successional BSCs, such as cyanobacterial crusts, to well-developed BSCs, such as lichen and moss crusts, has not yet been proposed. Few papers have analysed the changes in spectral characteristics when BSCs are disturbed by the common activities of livestock grazing and recreational use (resulting in trampling and/or scraping). As far as we know, only the work by Ustin *et al.* (2009) deals with this topic, demonstrating the potential for spectral detection of BSCs following experimentally controlled increases in summer precipitation, dry nitrogen deposition and mechanical disturbance by walking.

The objective of the present paper was twofold: (i) to demonstrate the efficiency of quantitative Vis-NIR spectral analysis in discriminating vegetation, physical crusts and various developmental stages of BSCs, and various types of disturbance to BSCs

and (ii) to develop a classification system for vegetation, physical crusts and the various developmental stages of BSCs, applicable in a variety of semiarid ecosystems.

Materials and methods

Study area

Spectra were acquired in two semiarid areas in southeast Spain, El Cautivo, located in the Tabernas Desert (N37°00'37", W2°26'30"), and Las Amoladeras, in Cabo de Gata-Níjar Natural Park (N36°48'34", W2°16'6"), both in Almería province.

The Tabernas Desert consists of a 'badland' catchment over gypsiferous-calcareous mudstones with an annual precipitation of 235 mm and a mean annual temperature of 17.8°C. A large part of the total annual precipitation (31–55%) is recorded during the winter and the rest is distributed between spring and autumn. The soils are silty and thin, except in some valleys and pediments of hillslopes. The landscape is made up of asymmetric northwest–southeast valleys. The upper parts of northeast-facing slopes are covered by incipient soils (Endoleptic Regosol, FAO, 1998) with dense lichen crusts and scattered annual and perennial plants. The common perennial plants are *Macrochloa tenacissima* (L.) Kunth, *Helianthemum almeriense* Pau, *Genista umbellata* (L'Hér.) Poiret, *Lycium intricatum* Boiss., *Artemisia barrelieri* Besser, *Salsola genistoides* Juss. ex Poir. and *Euzomodendron bourgaeum* Cosson. Soils on the pediments are thicker (Haplic Calcisol) and covered by annual and perennial plants. The southwest-facing slopes are steeper (up to 70°), with hardly any soil development (Epileptic Regosol). The pediments are bare or scarcely covered by lichens or annual plants. In this area, all soil devoid of vegetation is crusted, either by physical crusts or BSCs, causing some landforms to be completely covered by physical crusts or BSCs, with the latter also present between shrubs. A detailed description of this study area is given in Cantón *et al.* (2002, 2003).

Las Amoladeras is located approximately 22 km east of the city of Almería. It consists of a flat caliche (carbonate-influenced) area in the distal part of an alluvial fan south of the Alhambra range. The climate is similar to El Cautivo with a mean annual rainfall of 200 mm and a mean annual temperature of 18°C. Soil texture is sandy loam and soils are thin (10 cm average thickness with a maximum thickness of about 30 cm), smooth and saturated with carbonates and have a moderate stone content. They are classified as Rendzic or Calcaric Leptosols and Luvic or Haplic Calcisols. The area is sparsely vegetated and is dominated by clumps of *Macrochloa tenacissima* (L.) Kunth and dwarf shrubs such as *Helianthemum almeriense* Pau, *Thymus hyemalis* Lange, *Lycium intricatum* Boiss., *Hammada articulata* (Moq.) O. Bold's & Vigo, *Lygeum spartum* L., *Salsola genistoides* Juss. ex Poir. and *Launaea lanifera* Pau. The soil surface covered by physical crusts is very limited and most of the soil between the shrubs is occupied by BSCs, which represent some 30% of the area. Trampling by grazing sheep and goats is frequent.

Characterization of the soil crusts

The soil crust types were classified on the basis of visual assessment of their cover, composition and colour, according to the classification proposed by Lázaro *et al.* (2008). The main crust types identified in El Cautivo were: (i) physical crusts (hereafter P), which form over the mudstone regolith and cover all bare soil in this area, (ii) BSCs with incipient colonization by cyanobacteria (hereafter IC), (iii) dark BSCs mainly dominated by cyanobacterial species (hereafter C), which, along with frequent small, dark lichens including *Collema spp.*, cover about 80–90% of the soil surface, while a physical crust (7–10%) and light-coloured lichens (2–12%) cover the rest and (iv) light-coloured lichen-dominated BSCs (hereafter L), consisting mainly of *Squamarina lentigera* (Weber) Poelt and *Diploschistes diacapsis* (Ach.) Lumbsch (about 70–90%), with some cyanobacteria (10–20%) and physical crust (3–10%). These three types of BSCs represent a transition from poorly- to well-developed BSCs (Lázaro *et al.*, 2008). Similar types of crusts were identified in Las Amoladeras, but at this site, very little area of the soil surface was covered by physical crusts, and the most common crust types were BSCs. Species composition of the BSCs was similar to those of El Cautivo, except that in Las Amoladeras moss was very frequent in the BSCs. Thus, three types of BSCs were identified: (i) cyanobacteria-dominated BSCs (C), where cyanobacteria covered approximately 60–85% with some patches of physical crust (10–20%) and moss (2–20%), (ii) mixed lichen-moss BSCs (Lm), where lichen cover (mainly *Squamarina lentigera* and *Diploschistes diacapsis*) represented about 50–65% and moss 30–40% and (iii) moss-dominated BSCs, where moss represented some 55–60% and the rest was covered by cyanobacteria (30%) and physical crust (2–10%).

Spectral measurements

Spectral measurements were conducted in plots (described below) covered by the different crust types identified in the previous section. Crust spectral response was examined in either an intact or undisturbed state and then 6 months after disturbance by foot trampling (800 steps distributed homogeneously on the plot) or removal with a scraper (hereafter scraping). Note that scraping entirely removed the crust, whereas trampling disrupted the crust but left the fragments in the plot. The 6-month interval was to allow for stabilization and reorganization of soil surface particles after a couple of rainfall events so that the soil surface conditions were comparable among plots. Only the undisturbed physical crusts were analysed as these form quickly after rainfall (within a few minutes following cessation of the disruption; Ben-Dor *et al.*, 2003). Furthermore, the changes in the surface conditions of such crusts after trampling or scraping were hardly visible.

Spectra were acquired using a GER 2600 portable spectroradiometer (Spectra Vista Corporation, Poughkeepsie, New York, USA) with an optical resolution of 0.5 nm between 350 and 1000 nm and a resolution of 11.5 nm between 1000 and 2500 nm. Spectral measurements were made between 12.00 and 16.00 local

time during a 5-day period in February 2008, under clear sky conditions following a rain-free period of 2 weeks. *In situ* soil-moisture sensors indicated water contents of approximately 7% in El Cautivo and 13% in Las Amoladeras at a depth of 4 cm. Surface reflectance measurements were taken with a fibreoptic tube (23° field of view, FOV), at a height of about 60 cm from the soil surface (ground IFOV approximately 0.20 m²) on plots (2 × 2 m) representing individual crust types subjected to replicates of the various treatments. About 10–15 replicate measurements were collected within each plot. Because the area of soil surface covered by physical crusts in Las Amoladeras was scarce, only a few reflectance spectra were acquired from this surface. The reflectance spectra of various plant species were also acquired at both sites. Each spectral measurement consisted of the computerized average of five individual spectra. Before measuring each plot, a white reference was obtained using a Spectralon^(r) panel to compute the reflectance factor. Data were acquired with GER 2600 Data Collection Software on a laptop connected to the spectroradiometer.

Data pretreatment

Because measurements were taken under field conditions, the spectral ranges between 350 and 400 nm and between 1752 and 2514 nm were affected by strong noise and were not considered further. Furthermore, the spectrum was divided into two parts, each with different spectral resolutions (400–1000 and 1000–1752 nm), and a cubic polynomial smoothing filter with a 17 bands-window size was applied to each part (Savitzky & Golay, 1964).

Statistical analysis

Spectral datasets are usually (near) multi-colinear because they often consist of a large number of highly correlated variables (the reflectance at every wavelength across the spectrum) and a small number of samples (Næs & Mevik, 2001). To tackle this problem, principal component analysis (PCA) and partial least squares regression (PLSR) can be used to compress the spectral information on to a smaller number of non-colinear variables termed principal components (PCs). The model structure of PCA and PLSR is (Næs *et al.*, 2002, Equation (1):

$$\mathbf{X} = \mathbf{TP}' + \mathbf{E} \quad (1)$$

$$\mathbf{y} = \mathbf{Tq} + \mathbf{f} \quad (2)$$

where \mathbf{X} is the matrix of predictor (column-centred) variables, \mathbf{y} is the vector of response, \mathbf{T} is the score matrix representing the new PCs, matrix \mathbf{P}' and vector \mathbf{q} are the loadings (weights) of the original variables on each PC, and matrix \mathbf{E} and vector \mathbf{f} are the residuals in \mathbf{X} and \mathbf{y} , respectively. These PCs are linear combinations of the original variables and the loadings that are orthogonal to each other. In PCA, the scores are calculated such that the first PC accounts for the largest variation in the data and has the

maximum variance of the scores, and the following PCs explain as much of the remaining variation as possible. While PCA is an unsupervised method and only the spectral data are considered, PLSR exploits both the predictor and the response variables to extract PCs that are maximizing the covariance between the scores and the response variables. Here we used PCA and PLSR in combination with linear discriminant analysis (LDA) on Vis-NIR spectral data to assess the extent to which it is possible to discriminate and predict both ground cover classes (vegetation, physical crusts and different developmental stages of BSCs) and the nature of disturbance (trampling or scraping) that we imposed upon the BSCs. Half of the spectra were randomly selected to create a training set and the rest were used as a test set. A PCA was run on the training set and the first two PCs explaining approximately 90% of the spectral variation were retained. Similarly, a PLSR was fitted to the training set using dummy variables representing the ground cover classes to predict. The optimal number of components (with a maximum of 10 components) was determined using leave-one-out cross-validation (Wehrens & Mevik, 2007). Then, an LDA was applied separately on the PC scores obtained by PCA or PLSR and the classification efficiency of both approaches (PCA-LDA and PLSR-LDA) was compared with the test set. A confusion matrix was created by counting the number of well and wrongly classified classes in the test set and the performance of the classification was assessed by calculating Cohen's Kappa coefficient. This procedure was applied to spectral data obtained from each study site individually and then for the two study sites together. Similarly, the same approach was applied to a subset of the data for undisturbed crusts and those that had been disturbed.

Based on the outcome of these analyses, several variables were defined from the raw spectral data for the vegetation, physical crusts and undisturbed BSCs. Their appropriateness for classification and mapping of various BSCs as well as their ability to distinguish between BSCs, physical crusts and vegetation was tested. The variables tested were the albedo or average reflectance (for the entire spectral region and for specific spectral regions), calculated as the square root of the sum of the squares of reflectance at every

wavelength; slopes were calculated as the difference in reflectance between two selected wavelengths divided by the spectral gap between these wavelengths. The spectral absorptions at specific wavelengths were computed by application of the continuum-removal (CR) technique (Clark & Roush, 1984), which allows normalization of reflectance spectra and comparison of individual absorption features from a common baseline. First, the convex hull of the spectrum was computed and the set of points on the hull (the local maxima) was connected by a straight line. The continuum-removal (CR) values were then computed by dividing the reflectance by the interpolated line. The two endpoints are on the hull and their value was therefore equal to 1.0. Values less than 1.0 indicated the presence of absorption features. The continuum-removal was computed using ENVI 4.5 (ITT VIS, Boulder, CO, USA).

All statistical analyses were carried out using R software version 2.12.2 (R Development Core Team, 2010) and in particular, the PLS package of Wehrens & Mevik (2007) for PLSR, Ade4 package of Chessel *et al.* (2004) for PCA and MASS package of Venables & Ripley (2002) for LDA.

Results and discussion

Reflectance of undisturbed crust types and vegetation

The number of measurements, mean reflectance and standard deviation for the various types of ground cover at 550, 680 and 750 nm are shown in Table 1. The spectral variability was greater for the BSCs than for physical crusts or vegetation. Only M crusts showed small variability in their spectral signal and a reflectance in the visible (Vis) bands that was very similar to that of vegetation. Vegetation showed a large variability in the NIR.

The bare P crusts showed the greatest reflectance across the spectrum (Figure 1). The BSCs presented an absorption peak at about 680 nm (from chlorophyll *a*), which was absent or very weak in the P crusts. Vegetation was characterized by a small reflectance in the Vis (from absorption by photosynthetic pigments) and a large reflectance in the NIR and a reflectance peak

Table 1 Number of measurements per type of ground cover (vegetation and undisturbed crust types) and mean and standard deviation of reflectance at three important wavelengths

Study area	Cover type	<i>n</i>	Mean reflectance \pm standard deviation		
			550 nm	680 nm	750 nm
El Cautivo	Vegetation	27	5.2 \pm 1.9	7.7 \pm 3.5	22.8 \pm 5.1
	Physical crust	40	27.1 \pm 0.9	34.3 \pm 1.3	34.6 \pm 1.3
	Incipient-cyanobacterial crust	30	21.2 \pm 2.3	28.0 \pm 3.1	34.8 \pm 3.2
	Cyanobacterial crust	50	12.9 \pm 2.3	21.7 \pm 4.0	26.3 \pm 4.7
	Lichen crust	60	17.6 \pm 4.2	23.8 \pm 5.8	28.6 \pm 6.5
Las Amoladeras	Vegetation	23	4.6 \pm 1.6	6.1 \pm 1.9	21.3 \pm 7.6
	Physical crust	9	14.0 \pm 1.6	26.9 \pm 2.2	29.2 \pm 2.3
	Cyanobacterial crust	45	9.2 \pm 3.0	17.4 \pm 6.2	25.7 \pm 8.1
	Mixed lichen-moss crust	60	11.5 \pm 3.7	16.2 \pm 5.8	32.7 \pm 5.4
	Moss crust	45	4.6 \pm 1.2	8.1 \pm 1.6	19.9 \pm 1.9

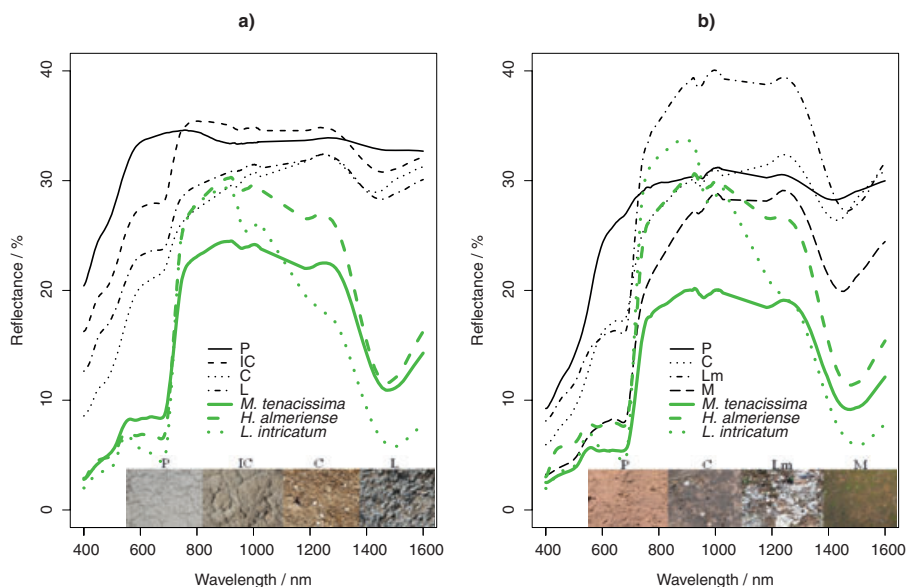


Figure 1 Mean reflectance spectra of different species of vegetation (*Macrochloa tenacissima*, *Helianthemum almeriense* and *Lycium intricatum*) and the types of soil crusts (C, cyanobacteria-dominated BSC; IC, incipient-cyanobacterial BSC; L, lichen-dominated BSC; Lm, mixed lichen-moss BSC; M, moss-dominated BSC; P, physical crust), at El Cautivo (a) and Las Amoladeras (b).

at 550 nm, which is absent in BSCs (Karnieli *et al.*, 1999; Chen *et al.*, 2005).

The spectral shapes of BSCs were similar but differed in their albedo, which decreased in the order $IC > L > C$ in El Cautivo, and $Lm > C > M$ in Las Amoladeras. An increase in reflectance from 400 to about 600 nm was observed followed by an absorption feature at about 680 nm. Between approximately 680 and 750 nm, there was a marked increase in the reflectance of all BSCs. The reflectance of the C and L crusts at El Cautivo continued to increase up to around 1220 nm, whereas that of IC crusts decreased slightly between approximately 750 and 980 nm, and then increased slightly up to about 1220 nm (Figure 1a). Beyond this wavelength, reflectance decreased until it reached a minimum at approximately 1450 nm, which was caused by absorption by water. The same features were observed in spectra obtained from BSCs at Las Amoladeras, but the slopes between approximately 680 and 750 nm and between approximately 750 and 980 nm were much steeper (probably because of the presence of moss; Figure 1b). Weber *et al.* (2008) described the spectral curves of cyanobacteria-, lichen- and moss-dominated BSCs in a semiarid area and also found poor reflectance at about 400 nm, which gradually increased to 600 nm, fell to a local minimum at about 680 nm and showed a strong acclivity between 700 and 830 nm. The bulb-shaped feature at about 1000 nm was probably an artefact at the splice between the two sensors.

The absorption feature that appears in BSC spectra at approximately 680 nm has been described by several different authors (O'Neill, 1994; Karnieli & Sarafis, 1996; Karnieli *et al.*, 2003). Cyanobacteria are the first colonizers in the succession of BSCs under arid or semiarid conditions, and later, if conditions permit, lichens and mosses colonize (Belnap, 2006). As the cyanobacterial biomass increases and later-successional species appear, the consequent increase in chlorophyll *a* and coloured pigments increases the colouration of the soil surface (Belnap *et al.*, 2008).

As the crust darkens during development, the absorption features in the red wavelengths increase and reflectance decreases (Karnieli *et al.*, 1999; Chen *et al.*, 2005). Thus, the C crusts showed less reflectance than the IC crusts (Figure 1a). However, greater BSC development does not always imply a decrease in reflectance because it depends on crust composition. Later-successional lichen species such as *Squamaria lentigera* and *Diploschistes diacapsis*, common on gypsiferous soils in semiarid areas of the Mediterranean region (Martínez *et al.*, 2006), are light-coloured and therefore, show greater reflectance in the Vis than do cyanobacterial crusts. Thus, L and Lm crusts showed more reflectance than C crusts (Figure 1). The dark M crusts are later-successional BSCs, and showed the least reflectance (Figure 1b).

Continuum-removal values of undisturbed crust types and vegetation

Continuum-removed reflectance values showed absorption features at approximately 500, 680 and 1450 nm, which were more intense for vegetation than for BSCs and very weak or absent for physical crusts (Figure 2). Absorption features in the Vis were more intense for the BSCs from Las Amoladeras than those from El Cautivo (Figure 2), probably because of the greater pigment content of the crusts at Las Amoladeras, and a greater organic carbon (OC) and total N content (on average 19 and 1.76 g kg⁻¹, respectively, in the C crust in Las Amoladeras and 12 and 1.71 g kg⁻¹, respectively, in El Cautivo; unpublished data). In El Cautivo, the absorption at about 680 nm (from chlorophyll *a*) was similar among the BSCs (mean CR at about 680 nm was 0.88 ± 0.04 in IC crusts, 0.92 ± 0.01 in C and 0.90 ± 0.02 in L), whereas the absorption at approximately 500 nm was more pronounced in the C crusts (mean CR 0.87 ± 0.01) than in the other BSCs (mean CR in the IC and L crusts was 0.94 ± 0.02) (Figure 2a). This absorption feature

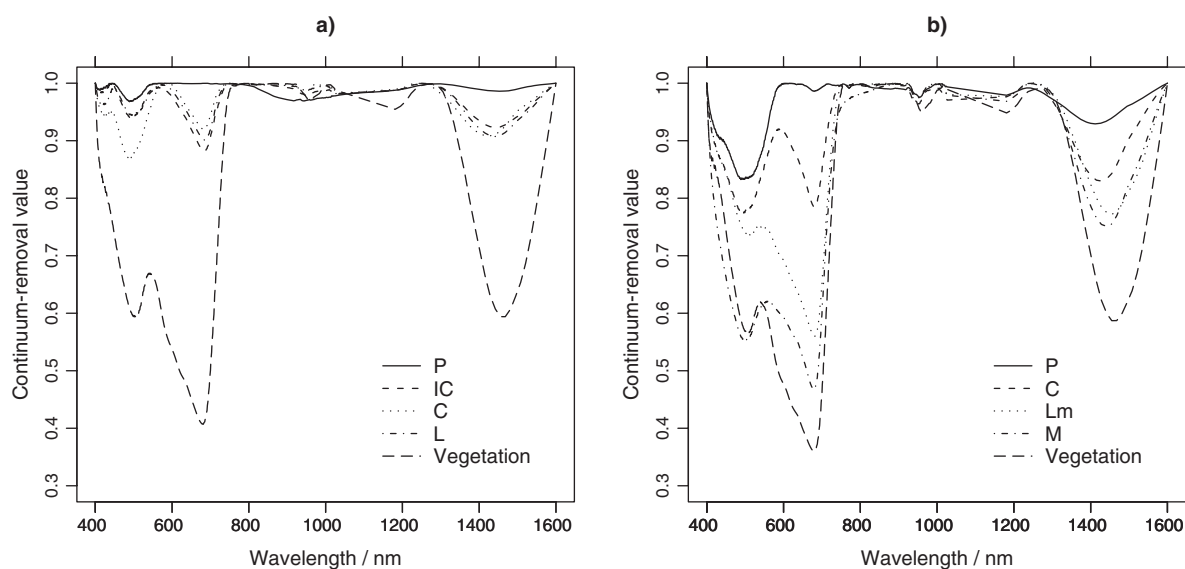


Figure 2 Mean spectra (continuum-removed) of vegetation and the various crust types, at El Cautivo (a) and Las Amoladeras (b) (C, cyanobacteria-dominated BSC; IC, incipient-cyanobacterial BSC; L, lichen-dominated BSC; Lm, mixed lichen-moss BSC; M, moss-dominated BSC; P, physical crust).

at approximately 500 nm could be attributed to the presence of carotenoid pigments, which absorb light between 400 and 500 nm (Weber *et al.*, 2008). One of the functions of carotenoids is to protect the photosynthetic system from excess UV radiation. Carotenoids are often formed in cyanobacteria in response to high light intensities, temperature and other stress factors (Reuter & Müller, 1993).

While cyanobacteria could employ carotenoids, as well as other pigments and metabolites, as a protection against excess light, the main mechanism of lichens for decreasing the influx of ultraviolet radiation is Ca oxalate crystals or calcite in the cortex of the mycobiont (Dietz *et al.*, 2000). This might explain why the absorption by L crusts at 500 nm was not as intense as by C crusts, despite them being more developed. In Las Amoladeras (Figure 2b), CR values at about 500 and about 680 nm increased from P crusts towards the most developed BSCs (thus $P < C < Lm < M$). This could be attributed to increased BSC development and moss cover. The absorption feature observed at about 680 nm for P crusts was probably caused by very early colonization by cyanobacteria. This was difficult to detect visually.

Absorption by water at about 1450 nm was more intense in the spectra of vegetation than those of BSCs. Wang *et al.* (2009) used this absorption feature as an estimation of plant water content. This absorption was more intense in spectra of BSCs at Las Amoladeras than in those at El Cautivo, because soil moisture was greater at Las Amoladeras at the time the spectra were collected. In general, Las Amoladeras undergoes less hydrological stress than El Cautivo because of its proximity (about 1 km) to the Mediterranean Sea. Absorption by water was similar in extent in all BSC spectra at El Cautivo, whereas it was more intense in Lm and M spectra than in C type BSCs at Las Amoladeras. Verrecchia *et al.* (1995) suggested that BSCs contribute to the retention of soil moisture.

This is supported by Cantón *et al.* (2004), who found reduced soil moisture content under physical soil crust surfaces compared with lichen-covered soil in El Cautivo. Our findings suggest that the spectral features associated with water may assist discrimination of BSCs and physical crusts.

Effects of disturbance on the spectral characteristics of BSCs

As the presence of BSCs usually darkens the soil, trampling and scraping caused an increase in albedo. Trampling and scraping the crust also flattened the soil surface, causing an increase in reflectance from a decrease in light-scattering and shadow-hiding effects (Matthias *et al.*, 2000). The reflectance was greater when the crust was scraped than when it was trampled (Figure 3). This difference is explained by the fact that scraping entirely removed the crust, whereas trampling caused a breakdown of the crust but left fragments on the plot, conferring increased roughness and darker colour to the soil and thus decreasing the albedo. Trampling had a stronger effect on reflectance in El Cautivo than in Las Amoladeras. The latter site suffers from frequent trampling by livestock and therefore the spectral response arising from further trampling is reduced. The spectral curves were especially similar for the undisturbed and trampled crusts in Las Amoladeras in the spectral region between approximately 700 and 1300 nm (Figure 3b).

Absorption by pigments at about 500 and about 680 nm and by water at about 1450 nm was strongest in the undisturbed crusts, somewhat weaker in the trampled crusts and weakest in the scraped crusts. Absorption by chlorophyll *a* in the scraped plots probably results from early colonization of these soils by

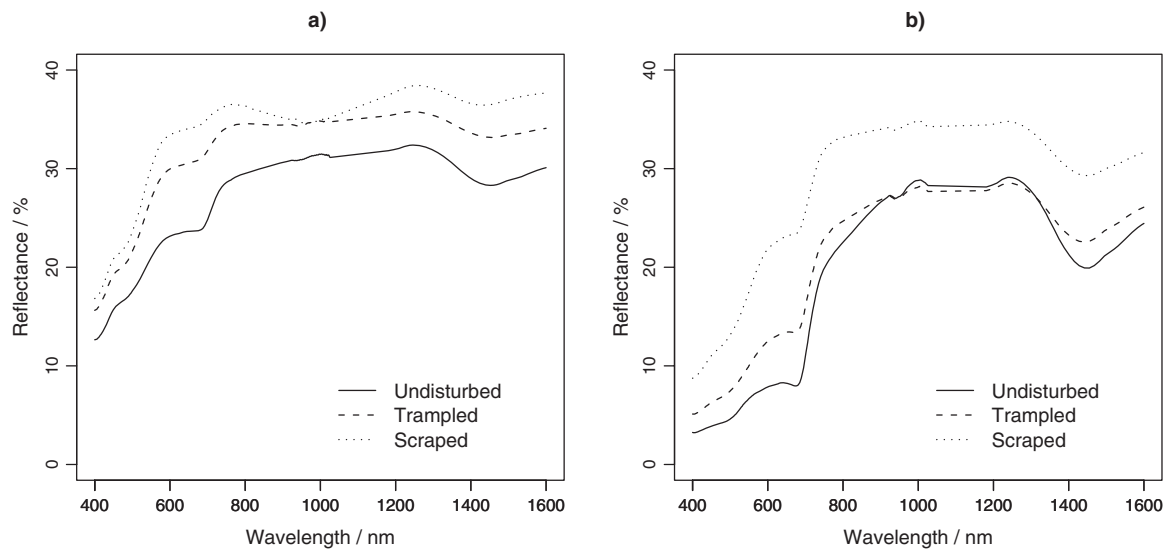


Figure 3 Mean reflectance spectra of the lichen-BSC at El Cautivo (a) and the moss-dominated BSC at Las Amoladeras (b) before and after scraping or trampling.

cyanobacteria during the 6 months between scraping and acquisition of spectra. The reflectance slope at wavelengths between approximately 750 and 980 nm in spectra from trampled and scraped plots and P and IC (undisturbed) crusts was generally small and decreasing or nearly zero, whereas it was increasing and steep in spectra for the well-developed BSCs. This suggests that this spectral slope steepens as later-successional species colonize and promote development of these crusts. This slope might therefore be used as an indicator of successional dynamics of BSCs. Zaady *et al.* (2007) demonstrated the possibility of using the normalized difference vegetation index (NDVI) as an indicator of successional trends of BSCs following disturbance, but suggested that its reliability during the wet season, when microphytes are active, would exceed that during the dry season. Ustin *et al.* (2009) reported that cover of BSCs was proportional to the CR values between 2010 and 2140 nm. They found the least absorption in plots with decreased BSC cover as a consequence

of increased summer irrigation and trampling treatments, and the most intensive in spectra from control plots of undisturbed BSCs.

Discrimination of undisturbed and disturbed crusts

Compared with PCA-LDA, spectral data processing using PLSR-LDA improved discrimination between vegetation and the different (undisturbed) crust types on the one hand and the various crust disturbances on the other hand, as assessed by values of the Kappa coefficient close to 1.0 (Kappa coefficients were greater than 0.90 in most cases, Table 2). A Kappa coefficient of 1.0 implies perfect agreement between the measured and predicted classes (types of ground cover), whereas values close to zero indicate poor agreement.

The PLSR-LDA applied to the training set showed a very good discrimination between vegetation and the various crust types for each site separately. The confusion matrix comparing the predicted and observed classes in the test set indicated that all types

Table 2 Kappa coefficients resulting from the confusion matrix after confronting the measured and predicted classes of the different ground covers and crust disturbance conditions (considering all crust types together and each crust type separately)

	El Cautivo					Las Amoladeras					Both sites
	Cover types	Crust disturbances (undisturbed, trampling, scraping)				Cover types	Crust disturbances (undisturbed, trampling, scraping)			Cover types	
		(Vegetation, P, IC, C, L)	All crust types (P, IC, C, L)	IC	C		L	(Vegetation, P, C, Lm, M)	All crust types (P, C, Lm, M)		
PCA-LDA	0.68	0.04	0.59	0.75	0.41	0.70	0.53	0.64	0.88	1	0.53
PLSR-LDA	1	0.64	0.97	1	0.91	1	0.88	0.97	1	1	0.96

Kappa coefficients close to 1 indicate good agreement between the measured and predicted classes in the confusion matrix, whereas values close to 0 indicate poor agreement. C, cyanobacteria-dominated BSC; IC, incipient-cyanobacterial BSC; L, lichen-dominated BSC; Lm, mixed lichen-moss BSC; M, moss-dominated BSC; P, physical crust.

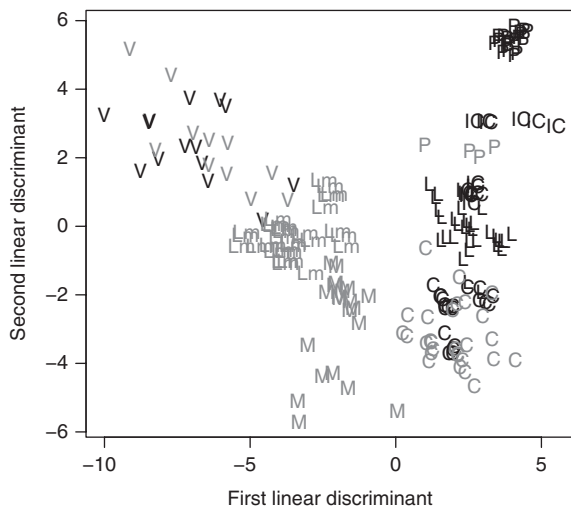


Figure 4 Classification of vegetation (V) and the undisturbed crust types (C, cyanobacteria-dominated BSC; IC, incipient-cyanobacterial BSC; L, lichen-dominated BSC; Lm, mixed lichen-moss BSC; M, moss-dominated BSC; P, physical crust) arising from LDA of PC scores extracted by PLSR, for the two study sites combined, where black and grey symbols indicate the corresponding surface types at El Cautivo and Las Amoladeras, respectively.

of ground cover were appropriately classified for each site (Kappa coefficient = 1.0, Table 2). As can be seen in Figure 4, application of PLSR-LDA to the training set for both sites combined also grouped the same types of ground cover together. The P crusts from Las Amoladeras appeared to be similar to the IC crusts from El Cautivo. This may arise from early colonization of these physical crusts by cyanobacteria (as supported by the small absorption feature at about 680 nm in the P crusts at Las Amoladeras, Figure 2b). The Kappa coefficient (0.96) obtained in the confusion matrix from comparison of the predicted and observed classes in the test site for both sites combined (Table 2) indicated a reliable classification.

The loadings of the first two PLSR PCs as a function of wavelength indicated the relative contribution of the wavelengths in the constructed PCs for data from El Cautivo, Las Amoladeras and the two sites combined. In El Cautivo (data not shown), the first PC, explaining 86% of the variance, had the greatest loading values at approximately 680–1450 nm, corresponding with absorption by chlorophyll *a* and water, respectively. The second PC accounted for 8% of the variance and the largest loadings occurred at about 500 nm, and were probably related to absorptions by carotenoids. At Las Amoladeras (data not shown), the first PC accounted for 82% of the variance in reflectance, and large absolute loading values were found throughout the NIR, probably caused by differences in albedo in this region of the spectrum. The second PC accounted for 15% of the variance in reflectance, with the largest loading values in the region between approximately 680 and 1000 nm, probably because of absorption by chlorophyll *a* and differences in the slopes between 680 and 750 nm, and 750 and 980 nm, and at wavelengths near 1450 nm because of

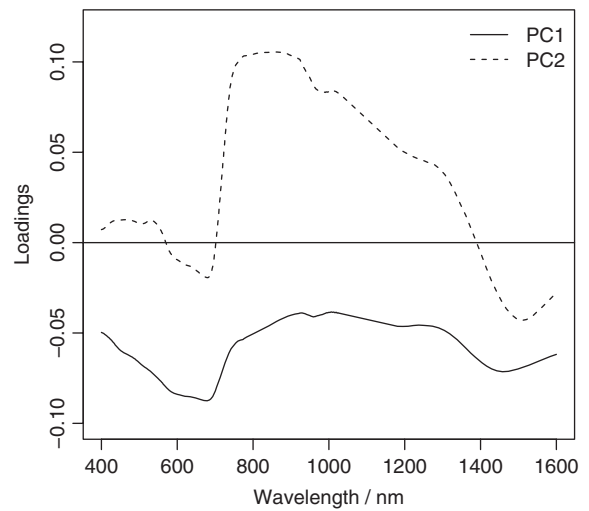


Figure 5 Loadings of the first two PCs as a function of wavelength following application of PLSR to spectra of the various types of ground cover for the two study sites combined.

absorption by water. The loadings of the first two PLSR PCs for both sites combined as a function of wavelength are shown in Figure 5. The first PC accounted for 78% of the total variance in reflectance and the largest absolute loadings were found at about 680–1450 nm (similarly to the first PC at El Cautivo). The second PC accounted for 10% of the variance in reflectance, with the highest absolute loadings in the region between approximately 680 and 1000 nm and at about 1450 nm (in a similar way to the second PC at Las Amoladeras).

Application of PLSR-LDA to training sets including spectra from undisturbed and disturbed crusts for each site separately indicated reasonable resolution of undisturbed, trampled and scraped crusts at each site (Table 2). The classification of all crust types at El Cautivo indicated some overlap for those scraped and trampled (Figure 6a). This overlap was reduced when data for an individual crust type were processed and scraping was clearly distinguishable from trampling (Figure 6b). The loadings of the first PLSR PC, accounting for 92% of the total variance, showed large values throughout the spectrum, probably related to the albedo. The same procedure applied to spectral data from Las Amoladeras showed that the first PC accounted for 77% of the variance in reflectance, with the largest loadings at about 680 and about 1450 nm. The second component accounted for 21% of the variance, with the largest loadings in the region between approximately 750 and 1300 nm (data not shown).

Although there have been attempts to predict soil physical, chemical and biological properties using Vis-NIR reflectance spectroscopy (Cécillon *et al.*, 2009a), and PCA and PLSR of Vis-NIR spectra have been used to assess soil quality (Cécillon *et al.*, 2009b), to our knowledge, these quantitative analyses have not been used to discriminate the developmental stages of soil crusts and disturbances to them as a prerequisite for a quantitative approach to mapping crust types in arid and semiarid areas.

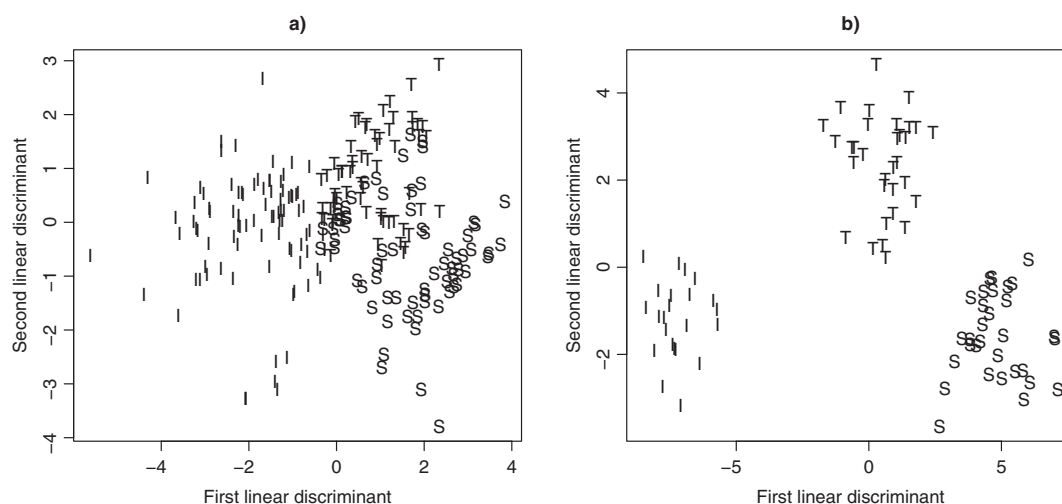


Figure 6 Classification of crust disturbances (I, intact; S, scraped; T, trampled) at El Cautivo after applying PLSR-LDA, considering all the crust types (a) and only the C crust (b).

A classification system to separate crust types

Some indices have been developed to distinguish BSCs from bare soil and plants (Karnieli, 1997; Chen *et al.*, 2005; Weber *et al.*, 2008). However, no index has yet been developed to discriminate different types of BSCs. From the outcome of a PLSR-LDA procedure on the spectral data, the CR value and slope variables

appeared to be useful in distinguishing the spectra from these different types of ground cover as illustrated by box plots in the following ways (Figure 7).

1. The CR value at about 1450 nm (CR1450) can be used to differentiate vegetation from physical crusts and BSCs (Figure 7a). As water content varies during the year, a more

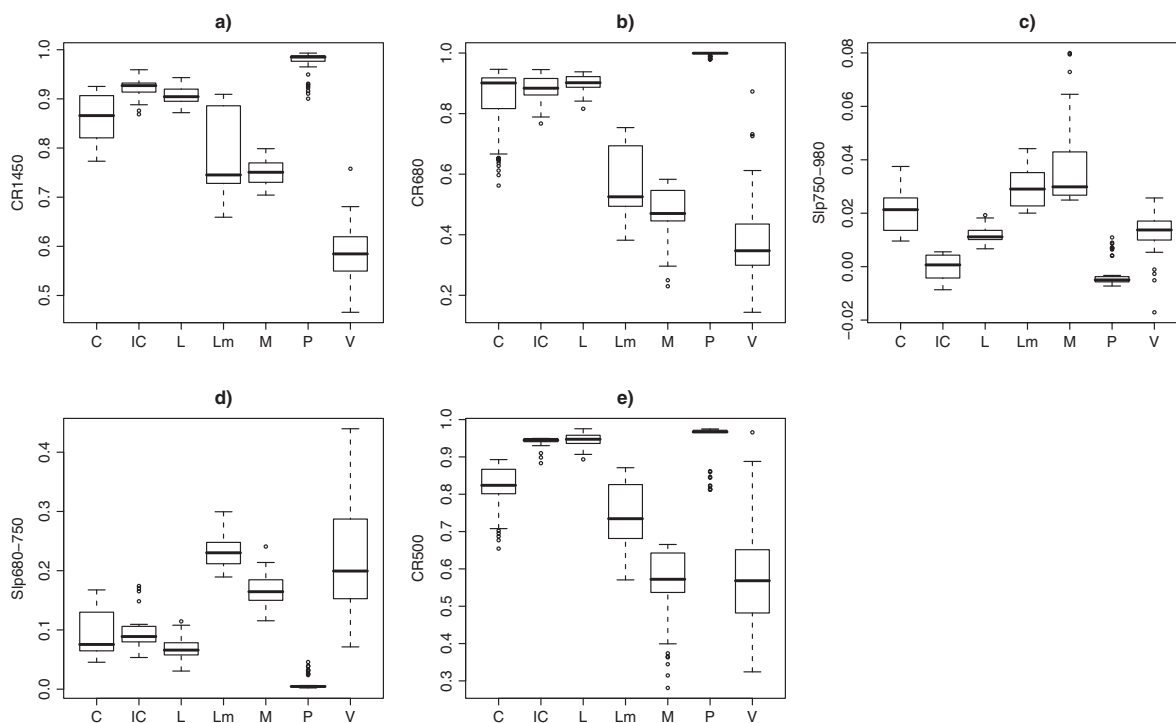


Figure 7 Box plots of the variables: (a) continuum-removal (CR) value at ~ 1450 nm, (b) CR value at ~ 680 nm, (c) slope between 680 and 750 nm, (d) slope between 750 and 980 nm, and (e) CR value at ~ 500 nm. The cover types are: vegetation (V) and the types of soil crusts (C, cyanobacteria-dominated BSC; IC, incipient-cyanobacterial BSC; L, lichen-dominated BSC; Lm, mixed lichen-moss BSC; M, moss-dominated BSC; P, physical crust).

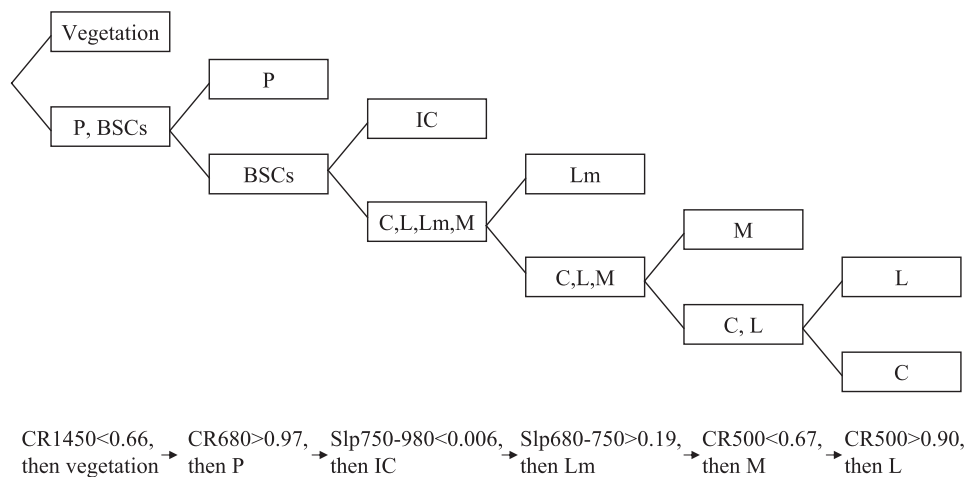


Figure 8 Decision tree for the classification of vegetation and the types of soil crusts (C, cyanobacteria-dominated BSC; IC, incipient-cyanobacterial BSC; L, lichen-dominated BSC; Lm, mixed lichen-moss BSC; M, moss-dominated BSC; P, physical crust).

detailed analysis of the relationship between water content and this spectral feature is of interest.

2. The CR value at about 680 nm (CR_{680}) (as well as that at CR_{1450} nm), can distinguish P crusts from BSCs (Figure 7b).
3. The slope between approximately 750 and 980 nm ($Slp_{750-980}$) allows ICs to be distinguished from other BSCs (Figure 7c).
4. The slope between approximately 680 and 750 nm ($Slp_{680-750}$) can be used to distinguish Lm from C, L and, to a large extent, M crusts (Figure 7d). Although the mean value for this variable was significantly greater in Lm than in M crusts, the distributions overlap. This appears to be reasonable because both have a significant cover of moss, which attenuates the underlying differences. Nevertheless, most of the samples of M and Lm crusts were correctly classified with this slope.
5. The CR value at about 500 nm (CR_{500}) allows C, L and M crusts to be distinguished (Figure 7e). Absorption by carotenoids followed the order $M > C > L$.

These observations provide a classification scheme distinguishing the various types of ground cover (Figure 8), which when applied to the complete dataset resulted in a Kappa coefficient of 0.96, suggesting a reasonable degree of reliability.

Conclusions

Quantitative analysis of the spectral characteristics of soil crusts demonstrates that some of these may be used to differentiate both cover type (vegetation, physical crusts and developmental stages of BSCs) and types of disturbance to BSCs. In general, as BSC development progresses, the crust darkens and its reflectance in the Vis decreases. However, late-successional L and Lm crusts were colonized by light-coloured lichen species, and consequently, these BSCs showed greater reflectance than

less developed ones. Scraping BSCs increased their reflectance to a greater extent than trampling. Our data suggest that the negative or slightly flat slope between about 750 and 980 nm in spectra of physical crusts or incipient BSCs becomes positive and steeper as the crust is colonized by late-successional species. Changes in this feature over time may be an indicator of succession dynamics as BSCs develop and/or of various disturbances to their surfaces. This may allow both temporal and spatial mapping to assess soil aggradation and degradation in arid regions.

This study has demonstrated that reflectance spectroscopy provides a tool for objective measurement of soil crust development. In this respect, spectral sensing may constitute an alternative to visual assessment. The differences between the spectral features in vegetation, physical crusts and various types of BSCs provide the basis for a classification index based on absorption features at approximately 500, 680 and 1450 nm, and the slopes between approximately 680 and 750 nm and between approximately 750 and 980 nm. The application of the proposed index to multispectral or hyperspectral images with a suitable spectral and spatial resolution could be a powerful tool for mapping different types of BSCs in semiarid areas. The future challenge is to assess the efficacy and efficiency of this index for detecting and mapping distribution of BSCs.

Acknowledgements

This work has been supported by the projects PROBASE (CGL2006-11619/HID) and BACARCOS (CGL2011-29429), both funded by the Ministerio de España de Ciencia e Innovación and including European Regional Development Funds (ERDF), and the project COSTRAS (RNM-3614), funded by the Consejería de Innovación y Ciencia de la Junta de Andalucía, including European Regional Development Funds (ERDF). The first author is funded by a FPI fellowship from the Spanish

Government (BES-2007-15218). Antoine Stevens is funded by the Fonds de Recherche Scientifique (F.R.S.-FNRS, Belgium). The support is gratefully acknowledged. We thank Cecilio Oyonarte and Paula Escribano for their guidance in the field design, Iván Ortiz for his help in the fieldwork and Monica García for her help in technical aspects. We thank David Tammadge for his revision of the language. An anonymous referee and the associate editor are kindly thanked for constructive comments on this manuscript.

References

- Belnap, J. 1995. Surface disturbances: their role in accelerating desertification. *Environmental Monitoring & Assessment*, **37**, 39–57.
- Belnap, J. 2006. The potential roles of biological soil crusts in dryland hydrologic cycles. *Hydrological Processes*, **20**, 3159–3178.
- Belnap, J., Phillips, S.L., Witwicki, D.L. & Miller, M.E. 2008. Visually assessing the level of development and soil surface stability of cyanobacterially dominated biological soil crusts. *Journal of Arid Environments*, **72**, 1257–1264.
- Ben-Dor, E., Goldshleger, N., Benyamini, Y., Agassi, M. & Blumberg, D.G. 2003. The spectral reflectance properties of soil's structural crust in the SWIR spectral region 1.2–2.5 μm . *Soil Science Society of America Journal*, **67**, 289–299.
- Ben-Dor, E., Goldshleger, N., Bonfil, D., Agassi, M., Margalit, N., Binayminy, Y. et al. 2004. Monitoring of infiltration rate in semi-arid soils using airborne hyperspectral technology. *International Journal of Remote Sensing*, **25**, 1–18.
- Cantón, Y., Domingo, F., Solé-Benet, A. & Puigdefábregas, J. 2002. Influence of soil surface types on the overall runoff of the Tabernas badlands (SE Spain). Field data and model approaches. *Hydrological Processes*, **16**, 2621–2643.
- Cantón, Y., Solé-Benet, A. & Lázaro, R. 2003. Soil–geomorphology relations in gypsiferous materials of the Tabernas desert (Almería, SE Spain). *Geoderma*, **115**, 193–222.
- Cantón, Y., Solé-Benet, A. & Domingo, F. 2004. Temporal and spatial patterns of soil moisture in semiarid badlands of SE Spain. *Journal of Hydrology*, **285**, 199–214.
- Cantón, Y., Solé-Benet, A., de Vente, J., Boix-Fayos, C., Calvo-Cases, A., Asensio, C. et al. 2011. A review of runoff generation and soil erosion across scales in semiarid south-eastern Spain. *Journal of Arid Environments*, **75**, 1254–1261. doi: 10.1016/j.jaridenv.2011.03.004.
- Cécillon, L., Barthès, B.G., Gomez, C., Ertlen, D., Genot, V., Hedde, M. et al. 2009a. Assessment and monitoring of soil quality using near-infrared reflectance spectroscopy (NIRS). *European Journal of Soil Science*, **60**, 770–784.
- Cécillon, L., Cassagne, N., Czarnes, S., Gros, R., Vennetier, M. & Brun, J.J. 2009b. Predicting soil quality indices with near infrared analysis in a wildfire chronosequence. *Science of the Total Environment*, **407**, 1200–1205.
- Cerdan, O., Souchère, V., Lecomte, V., Couturier, A. & Le Bissonnais, Y. 2001. Incorporating soil surface crusting processes in an expert based runoff model: sealing and transfer by runoff and erosion related to agricultural management. *Catena*, **46**, 189–205.
- Chen, J., Zhang, M.Y., Wang, L., Shimazaki, H. & Tamura, M. 2005. A new index for mapping lichen-dominated biological soil crusts in desert areas. *Remote Sensing of Environment*, **96**, 165–175.
- Chessel, D., Dufour, A.B. & Thioulouse, J. 2004. The ade4 package—I: one-table methods. *R News*, **4**, 5–10.
- Clark, R.N. & Roush, T.L. 1984. Reflectance spectroscopy. Quantitative analysis techniques for remote sensing applications. *Journal of Geophysical Research*, **89**, 6329–6340.
- Dietz, S., Büdel, B., Lange, O.L. & Bilger, W. 2000. Transmittance of light through the cortex of lichens from contrasting habitats. *Bibliotheca Lichenologica*, **75**, 171–182.
- FAO 1998. *World Reference Base for Soil Resources*. World Soil Resources Report No 84, FAO, Rome.
- Karnieli, A. 1997. Development and implementation of spectral crust index over dune sands. *International Journal of Remote Sensing*, **18**, 1207–1220.
- Karnieli, A. & Sarafis, V. 1996. Reflectance spectrometry of cyanobacteria within soil crusts—a diagnostic tool. *International Journal of Remote Sensing*, **8**, 1609–1615.
- Karnieli, A., Kidron, G.J., Glaesser, C. & Ben-Dor, E. 1999. Spectral characteristics of cyanobacteria soil crust in semiarid environments. *Remote Sensing of Environment*, **69**, 67–75.
- Karnieli, A., Kokaly, R.F., West, N.E. & Clark, R.N. 2003. Remote sensing of biological soil crusts. In: *Biological Soil Crusts: Structure, Function, and Management* (eds J. Belnap & O.L. Lange), pp. 431–455. Springer-Verlag, Berlin, Heidelberg.
- King, C., Baghdadi, N., Lecomte, V. & Cerdan, O. 2005. The application of remote-sensing data to monitoring and modelling of soil erosion. *Catena*, **62**, 79–93.
- Lázaro, R., Cantón, Y., Solé-Benet, A., Bevan, J., Alexander, R., Sancho, L.G. et al. 2008. The influence of competition between lichen colonization and erosion on the evolution of soil surfaces in the Tabernas badlands (SE Spain) and its landscape effects. *Geomorphology*, **102**, 252–266.
- Maestre, F.T., Bowker, M.A., Cantón, Y., Castillo-Monroy, A.P., Cortina, J., Escolar, C. et al. 2011. Ecology and functional roles of biological soil crusts in semi-arid ecosystems of Spain. *Journal of Arid Environments*, **75**, 1282–1291. doi: 10.1016/j.jaridenv.2010.12.008.
- Martínez, I., Escudero, A., Maestre, F.T., de la Cruz, A., Guerrero, C. & Rubio, A. 2006. Small-scale patterns of abundance of mosses and lichens forming biological soil crusts in two semi-arid gypsum environments. *Australian Journal of Botany*, **54**, 339–348.
- Matthias, A.D., Fimbres, A., Sano, E.E., Post, D.F., Accioli, L., Batchily, A.K. et al. 2000. Surface roughness effects on soil albedo. *Soil Science Society of America Journal*, **64**, 1035–1041.
- Næs, T. & Mevik, B.H. 2001. Understanding the collinearity problem in regression and discriminant analysis. *Journal of Chemometrics*, **15**, 413–426.
- Næs, T., Isaksson, T., Fearn, T. & Davies, T. 2002. *A User Friendly Guide to Multivariate Calibration and Classification*. NIR Publications, Chichester.
- O'Neill, A.L. 1994. Reflectance spectra of microphytic soil crusts in semi-arid Australia. *International Journal of Remote Sensing*, **15**, 675–681.
- R Development Core Team 2010. *R: A Language and Environment for Statistical Computing*. R Foundation for Statistical Computing, Vienna [WWW document]. URL <http://www.R-project.org> [accessed on 18 March 2011].
- Reuter, W. & Müller, C. 1993. New trends in photobiology: adaptation of the photosynthetic apparatus of cyanobacteria to light and CO₂. *Journal of Photochemistry & Photobiology*, **21**, 3–27.

- Savitzky, A. & Golay, M.J.E. 1964. Smoothing and differentiation of data by simplified least squares procedures. *Analytical Chemistry*, **36**, 1627–1639.
- Ustin, S.L., Valko, P.G., Kefauver, S.C., Santos, M.J., Zimpfer, J.F. & Smith, S.D. 2009. Remote sensing of biological soil crust under simulated climate change manipulations in the Mojave Desert. *Remote Sensing of Environment*, **113**, 317–328.
- Venables, W.N. & Ripley, B.D. 2002. *Modern Applied Statistics with S*. Springer, New York.
- Verrecchia, E., Yair, A., Kidron, G.J. & Verrecchia, K. 1995. Physical properties of the psammophile cryptogamic crust and their consequences to the water regime of sandy soils, north–western Negev Desert, Israel. *Journal of Arid Environments*, **29**, 427–437.
- Wang, J., Xu, R. & Yang, S. 2009. Estimation of plant water content by spectral absorption features centered at 1,450 nm and 1,940 nm regions. *Environmental Monitoring & Assessment*, **157**, 459–469.
- Weber, B., Olehowski, C., Knerr, T., Hill, J., Deutschewitz, K., Wessels, D.C.J. *et al.* 2008. A new approach for mapping of biological soil crusts in semidesert areas with hyperspectral imagery. *Remote Sensing of Environment*, **112**, 2187–2201.
- Wehrens, R. & Mevik, B.H. 2007. The pls package: partial least squares regression (PLSR) and principal component regression (PCR). R package version 2.1-0 URL: <http://mevik.net/work/software/pls.html> [accessed on 15 November 2010].
- Zaady, E., Karnieli, A. & Shachak, M. 2007. Applying a field spectroscopy technique for assessing successional trends of biological soil crusts in a semi-arid environment. *Journal of Arid Environments*, **70**, 463–477.
- Zhan, X.C. & Miller, P.C. 1996. Physical and chemical crusting processes affecting runoff and erosion in Furrows. *Soil Science Society of America Journal*, **60**, 860–865.